

A&A manuscript no.
(will be inserted by hand later)

Your thesaurus codes are:
08 (08.03.4; 08.05.2; 08.09.2: AB Aur, HD 163296; 08.16.5; 13.09.6)

ASTRONOMY
AND
ASTROPHYSICS

ISO spectroscopy of circumstellar dust in the Herbig Ae systems AB Aur and HD 163296 [★]

M.E. van den Ancker^{1,2}, J. Bouwman¹, P.R. Wesselius³, L.B.F.M. Waters^{1,4}, S.M. Dougherty^{5,6}, and E.F. van Dishoeck⁷

¹ Astronomical Institute “Anton Pannekoek”, University of Amsterdam, Kruislaan 403, NL–1098 SJ Amsterdam, The Netherlands

² Harvard-Smithsonian Center for Astrophysics, 60 Garden Street, MS 42, Cambridge MA 02138, USA

³ SRON Laboratory for Space Research Groningen, P.O. Box 800, NL–9700 AV Groningen, The Netherlands

⁴ Instituut voor Sterrenkunde, Katholieke Universiteit Leuven, Celestijnenlaan 200B, B-3001 Heverlee, Belgium

⁵ Dept. of Physics & Astronomy, University of Calgary, 2500 University Drive NW, Calgary, Alberta T2N 1N4, Canada

⁶ Dominion Radio Astrophysical Observatory, P.O. Box 248, White Lake Road, Penticton, British Columbia V2A 6K3, Canada

⁷ Leiden Observatory, P.O. Box 9513, NL–2300 RA Leiden, The Netherlands

Received [date]; accepted [date]

Abstract. Using both the Short- and Long-wavelength Spectrometers on board the Infrared Space Observatory (ISO), we have obtained infrared spectra of the Herbig Ae systems AB Aur and HD 163296. In addition, we obtained ground-based *N* band images of HD 163296. Our results can be summarized as follows: (1) The main dust components in AB Aur are amorphous silicates, iron oxide and PAHs; (2) The circumstellar dust in HD 163296 consists of amorphous silicates, iron oxide, water ice and a small fraction of crystalline silicates; (3) The infrared fluxes of HD 163296 are dominated by solid state features; (4) The colour temperature of the underlying continuum is much cooler in HD 163296 than in AB Aur, pointing to the existence of a population of very large (mm sized) dust grains in HD 163296; (5) The composition and degree of crystallization of circumstellar dust are poorly correlated with the age of the central star. The processes of crystallization and grain growth are also not necessarily coupled. This means that either the evolution of circumstellar dust in protoplanetary disks happens very rapidly (within a few Myr), or that this evolution is governed by factors other than stellar mass and age.

Key words: Circumstellar matter – Emission-line stars – Stars: AB Aur, HD 163296 – Pre-main sequence stars – Infrared: Stars

1. Introduction

Herbig Ae/Be stars are intermediate-mass pre-main sequence stars surrounded by disks of gas and dust which might be the site of on-going planet formation (see Waters & Waelkens 1998

for a recent review). AB Aur (A0Ve) and HD 163296 (A3Ve) belong to the best studied Herbig stars and are sometimes considered prototypical for the entire class. As early as 1933, Merrill & Burwell remarked upon the similarity of both systems, which was confirmed by numerous subsequent authors. Apart from the fact that the stellar mass, effective temperature and age of AB Aur and HD 163296 are nearly identical (van den Ancker et al. 1997, 1998), the similarity between the two systems also extends to their circumstellar environment: both AB Aur and HD 163296 are examples of relatively isolated star formation, and are not hindered by confusion with other sources (Henning et al. 1998; Di Francesco et al. 1998).

Both AB Aur and HD 163296 show a rich, variable, emission-line spectrum from the ultraviolet to the optical. With a few exceptions, most noticeably the observed [O I] emission, these lines have been successfully modelled as arising in an inhomogeneous stellar wind (Catala et al. 1989; Böhm et al. 1996; Bouret et al. 1997). Infall of material has been detected in both HD 163296 and AB Aur through monitoring of UV and optical absorption and emission lines and can be explained by the presence of infalling evaporating exocomets (Grady et al. 1996, 1999). In the infrared, both stars are among the sources with the strongest 10 μ m silicate feature in emission (Cohen 1980; Sitko 1981; Sorrell 1990). Sitko et al. (1999) compared the 10 μ m silicate feature in HD 163296 with that of solar-system comets and found a striking resemblance with that of comet Hale-Bopp. Neither star shows the 3.29 μ m UIR emission band present toward many Herbig Ae/Be stars (Brooke et al. 1993; Sitko et al. 1999). Basic astrophysical parameters of both stars are listed in Table 1.

There is strong evidence for the presence of a circumstellar disk in both AB Aur and HD 163296. Bjorkman et al. (1995) detected a 90° flip of the polarization angle between the optical and the ultraviolet in HD 163296, which they interpreted as evidence for a flattened, disk-like structure. Mannings & Sargent (1997) resolved the gaseous disks surrounding AB Aur and HD 163296 using CO millimeter wave aperture synthesis

Send offprint requests to: M.E. van den Ancker (mario@astro.uva.nl)

[★] Based on observations with ISO, an ESA project with instruments funded by ESA Member States (especially the PI countries: France, Germany, the Netherlands and the United Kingdom) and with the participation of ISAS and NASA and on observations collected at the European Southern Observatory, La Silla, Chile.

imaging. Using continuum measurements at 1.3 mm, the same authors also resolved the circumstellar dust disk of HD 163296. The AB Aur dust disk has also been resolved in the infrared, and shows a surprisingly strong dependence of disk diameter on wavelength, ranging from $0''.0065$ (0.94 AU) at $2.2 \mu\text{m}$ (Millan-Gabet et al. 1999), through $0''.24$ (35 AU) at $11.7 \mu\text{m}$ to $0''.49$ (70 AU) at $17.9 \mu\text{m}$ (Marsh et al. 1995).

In this paper we present new infrared spectra of AB Aur and HD 163296 obtained with the Short- and Long Wavelength Spectrometers on board the *Infrared Space Observatory* (ISO; Kessler et al. 1996). We will discuss these spectra and their implications for the evolution of dust in Herbig systems. In a subsequent paper (Bouwman et al. 2000), we will describe a model for the circumstellar dust disks of AB Aur and HD 163296 and apply it to these data.

2. Observations

ISO Short Wavelength ($2.4\text{--}45 \mu\text{m}$) Spectrometer (SWS; de Graauw et al. 1996) and Long Wavelength ($43\text{--}197 \mu\text{m}$) Spectrometer (LWS; Clegg et al. 1996) full grating scans of AB Aur were obtained in ISO revolutions 680 (at JD 2450717.747) and 835 (JD 2450872.380), respectively. An SWS full grating scan of HD 163296 was made in revolution 329 (JD 2450367.398). Observing times were 3666 seconds for the SWS and 2741 seconds for the LWS observations. Data were reduced in a standard fashion using calibration files corresponding to OLP version 7.0 (SWS) or 6.0 (LWS), after which they were corrected for remaining fringing and glitches. To increase the S/N in the final spectra, statistical outliers were removed and the detectors were aligned, after which the spectra were rebinned to a lower spectral resolution. The resulting spectra are shown in Fig. 1.

N-band ($10.1 \mu\text{m}$) images of HD 163296 were obtained on July 25, 1997 (at JD 2450654.608) using TIMMI on the ESO 3.6m telescope at La Silla. Total integration time was 65 minutes. The pixel size was $0''.336$, with a total field of view of $21''.5 \times 21''.5$. After a standard reduction procedure, the HD 163296 image was indistinguishable from that of the standard star η Sgr. After deconvolution of the HD 163296 image with that of η Sgr, the resulting stellar image stretched across 2 pixels. We conclude that the bulk of the $10 \mu\text{m}$ flux of HD 163296 comes from an area less than $0''.7$ (90 AU at 122 pc) in diameter.

3. Contents of spectra

The infrared spectra of AB Aur and HD 163296 (Fig. 1) show big differences: whereas AB Aur shows the cool, strong continuum expected for a Herbig star, for HD 163296 the continuum appears to be so weak that the entire SWS spectrum is dominated by solid-state emission features. The IRAS fluxes also plotted in Fig. 1 suggest that an underlying continuum in HD 163296 is present, but peaks longward of $100 \mu\text{m}$ and therefore is much cooler than the $\approx 40 \text{ K}$ continuum in AB Aur.

Table 1. Astrophysical parameters of programme stars

| | AB Aur | Ref. | HD 163296 | Ref. |
|-----------------------------------|-------------------------------|------|----------------------|------|
| α (2000) | 04 55 45.79 | (1) | 17 56 21.26 | (1) |
| δ (2000) | +30 33 05.5 | (1) | −21 57 19.5 | (1) |
| d [pc] | 144^{+23}_{-17} | (2) | 122^{+17}_{-13} | (2) |
| Sp. Type | A0Ve+sh | (3) | A3Ve | (8) |
| V [m] | $7.03\text{--}7.09^{\dagger}$ | (2) | $6.82\text{--}6.89$ | (2) |
| $E(B - V)$ [m] | 0.16 ± 0.02 | (4) | 0.04 ± 0.02 | (4) |
| T_{eff} [K] | 9500^{+500}_{-300} | (2) | 8700^{+200}_{-300} | (4) |
| L_* [L_{\odot}] | 47 ± 12 | (2) | 26 ± 5 | (4) |
| R_* [R_{\odot}] | 2.5 ± 0.5 | (4) | 2.2 ± 0.2 | (4) |
| M_* [M_{\odot}] | 2.4 ± 0.2 | (2) | 2.0 ± 0.2 | (4) |
| $\log(\text{Age})$ [yr] | 6.3 ± 0.2 | (2) | 6.6 ± 0.2 | (4) |
| H α | P Cygni | (5) | Double-peaked | (9) |
| $v \sin i$ [km s^{-1}] | 80 ± 5 | (5) | 120 ± 1 | (10) |
| rot. period [$^{\text{h}}$] | 32 ± 3 | (6) | 35 ± 5 | (11) |
| i [$^{\circ}$] | 76 | (7) | 58 | (7) |
| P.A. [$^{\circ}$] | $+79^{+2}_{-3}$ | (7) | $+126^{+2}_{-3}$ | (7) |

[†]However, older photographic measurements (Gaposchkin 1952) show values up to $m_{pg} = 8.4$ for AB Aur.

References: (1) Hipparcos Catalogue; (2) van den Ancker et al. (1998); (3) Böhm & Catala (1993); (4) This paper; (5) Böhm & Catala (1995); (6) Böhm et al. (1996); (7) Mannings & Sargent (1997); (8) Gray & Corbally (1998); (9) Pogodin (1994); (10) Halbedel (1996); (11) Catala et al. (1989).

Both AB Aur and HD 163296 show a strong $9.7 \mu\text{m}$ amorphous silicate feature in emission together with a broad emission complex ranging from 14 to $38 \mu\text{m}$. The emissivities for various dust components in the spectra are also included in Fig. 1. In the HD 163296 spectrum the broad emission complex ranging from 14 to $38 \mu\text{m}$ is too broad and too intense to be solely attributed to the $19 \mu\text{m}$ feature due to the O–Si–O bending mode. We tentatively attribute this feature to a blend of silicates and iron oxide. Lab spectra of FeO also show a strongly rising emissivity in the short-wavelength range of the SWS (Henning et al. 1995). When folded with a $\approx 800 \text{ K}$ blackbody, this naturally produces a broad emission feature peaking around 3 microns , which is present in both stars.

The large degree of redundancy in the SWS data makes it possible to assess the reality of weak spectral features which at first glance may appear to be lost in the noise. Each part of the spectrum was scanned twice by twelve detectors, so by checking whether a particular feature is seen in all detectors and in both scan directions, it is possible to disentangle real features from noise. The features identified in this way are listed in Table 2. AB Aur clearly shows the familiar 6.2 and 7.7 and possibly also the 8.6 and $11.2 \mu\text{m}$ UIR bands usually attributed to emission by polycyclic aromatic hydrocarbons (PAHs), as well as a new UIR band at $15.9 \mu\text{m}$. The $3.29 \mu\text{m}$ UIR band is absent.

The HD 163296 spectrum shows a number of small emission features at wavelengths corresponding to those of crystalline olivines ($(\text{Mg}_x\text{Fe}_{1-x})_2\text{SiO}_4$). Remarkably, the amor-

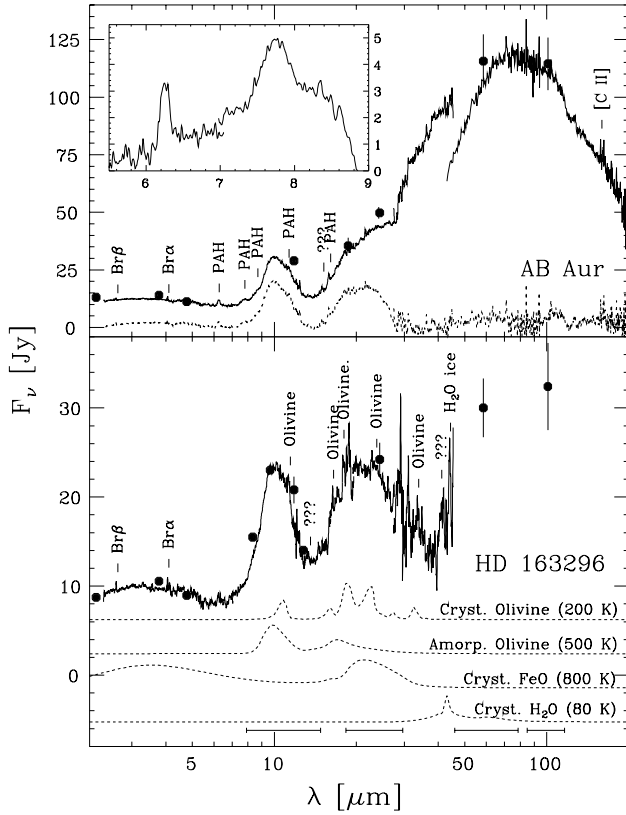


Fig. 1. ISO spectra of AB Aur (top) and HD 163296 (bottom) with the main features identified. The solid dots indicate ground-based and IRAS photometry (Berrilli et al. 1987, 1992; Hillenbrand et al. 1992; Weaver & Jones 1992). The dashed line in the top plot is the AB Aur spectrum after subtracting a spline fit to the continuum. Also shown (dashed lines at bottom) are the emissivities at a given temperature of the various dust components in the spectra (Jäger et al. 1998; Dorschner et al. 1995; Henning et al. 1995; Bertie et al. 1969). The bars at the bottom of the plot show the IRAS 12, 25, 60 and 100 μm passbands (FWHM). The inset in the AB Aur plot shows the UIR bands in the 5.5–9.0 μm region after subtracting a pseudo-continuum.

phous silicate feature has a higher band-strength relative to the continuum in our ISO data than in the ground-based 8–13 μm spectrum of HD 163296 by Sitko et al. (1999). In contrast, the 11.2 μm shoulder, due to crystalline silicates, appears weaker in our spectrum, suggesting a significant time variability of both components.

In addition to this, HD 163296 shows emission from the 44 μm H₂O ice feature. The relative location of the IRAS 60 μm measurement in comparison to the SWS spectrum suggests that the long-wavelength H₂O ice feature around 69 μm as well as the broad unidentified feature longward of 100 μm , observed in HD 100546 and HD 142527 (Malfait et al. 1998, 1999), might also be very prominent in HD 163296. PAHs are very weak or absent in HD 163296.

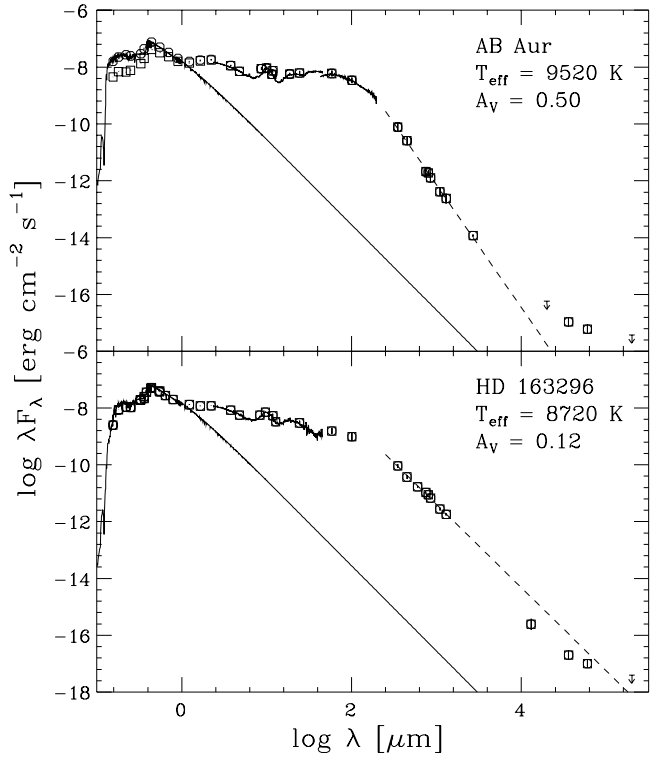


Fig. 2. Spectral energy distributions of AB Aur (top) and HD 163296 (bottom). Open squares and circles indicate observed and extinction corrected fluxes from literature (Wesselius et al. 1982; Thé et al. 1985; Strom et al. 1972; Cohen & Schwartz 1976; Berrilli et al. 1987, 1992; Hillenbrand et al. 1992; Weaver & Jones 1992; Mannings 1994; Güdel et al. 1989; Brown et al. 1993; Skinner et al. 1993). The solid lines show Kurucz models for the stellar photospheres of AB Aur and HD 163296. The dashed lines show linear fits to the submm data points for comparison with the slope of the Rayleigh-Jeans tail of the Kurucz model.

In addition to the solid-state features, both AB Aur and HD 163296 also contain a number of H I recombination lines at shorter wavelengths. All lines from the Bracket and Pfund included in the SWS wavelength range series are present, while the higher H I series are not detected, possibly due to the combined effect of a lower instrumental sensitivity and a higher background in this part of the spectrum. These recombination line data will be discussed in more detail in a forthcoming paper.

The LWS spectrum of AB Aur is relatively smooth and featureless. The only line that is clearly visible in the spectrum is the [C II] line at 157.7 μm . The strength of this line ($8.6 \times 10^{-16} \text{ W m}^{-2}$) is compatible with it originating in the background rather than being circumstellar. As can be seen from Fig. 1, there is a $\approx 25\%$ difference in the flux scales between the AB Aur SWS and LWS spectra in the overlapping region. Although within the formal errors of the absolute flux calibration for SWS and LWS, this discrepancy is larger than that found in other sources. The difference cannot be attributed to the dif-

Table 2. Contents of Spectra

| Feature λ [μm] | FeO [3] | PAH [3.3] | PAH [6.2] | PAH [7.7] | PAH [8.6] | Si-O [9.7] | PAH [11.2] | [15.0] | PAH [15.9] | O-Si-O [19] | FeO [23] |
|--|------------|--------------|--------------|--------------|--------------|---------------|---------------|--------|---------------|----------------|-------------|
| AB Aur | ✓ | – | ✓ | ✓ | ✓ | ✓ | ✓: | ✓: | ✓ | ✓ | ✓ |
| HD 163296 | ✓ | ✓: | ✓: | – | – | ✓ | – | – | – | ✓ | ✓ |

| Feature λ [μm] | Oliv. [11.3] | [13.4] | Oliv. [16.3] | Oliv. [17.8] | Pyr.? [18.2] | Oliv. [23.5] | Oliv. [31.3] | Oliv. [33.5] | [40.7] | H ₂ O ice [43.8] |
|--|-----------------|--------|-----------------|-----------------|-----------------|-----------------|-----------------|-----------------|--------|--------------------------------|
| AB Aur | – | – | – | – | – | – | ✓: | ✓: | ✓: | – |
| HD 163296 | ✓ | ✓ | ✓ | ✓ | ✓ | ✓ | ✓ | ✓ | ✓ | ✓ |

ferent aperture sizes ($33'' \times 20''$ for SWS versus a circular $80''$ FWHM for LWS), and confusion with extended emission, since then the LWS spectrum would have to have a higher flux level than the SWS spectrum. It is interesting to note that in the time interval between the SWS and LWS measurements, AB Aur did show an optical photometric event which could have also affected the infrared brightness (van den Ancker et al. 1999 and references therein), so the difference in flux between SWS and LWS might in fact be due to real variability. In Fig. 1 we also plotted the IRAS fluxes of AB Aur. Although compatible with both spectra, the IRAS $60 \mu\text{m}$ flux agrees better with the SWS spectrum, so we rather arbitrarily choose to adopt the SWS flux calibration for the region around $45 \mu\text{m}$.

4. Spectral energy distributions

Spectral Energy Distributions (SEDs) of AB Aur and HD 163296 were constructed from literature data as well as our new ISO spectra and newly obtained VLA photometry for HD 163296 and are shown in Fig. 2. All the submm fluxes in these SEDs refer to single-dish measurements. As can be seen from Fig. 2, the SED can be naturally decomposed in three parts: the optical wavelength range, where the total system flux is dominated by the stellar photosphere, the infrared to submm, where emission originates from the circumstellar dust disk, and the radio, where free-free emission from the stellar wind becomes dominant.

The difference in behaviour of the dust component in HD 163296 and AB Aur is striking: after a nearly flat energy distribution in the infrared, the sub-mm and mm fluxes of AB Aur drop rapidly ($\lambda F_\lambda \propto \lambda^{-4.3}$), indicative of the dust becoming optically thin at these wavelengths, whereas toward HD 163296 the slope of the sub-mm to mm fluxes ($\propto \lambda^{-2.9}$) is within errors equal to that of the Rayleigh-Jeans tail of a black body ($\propto \lambda^{-3}$). The new radio points at 1.3, 3.6 and 6 cm for HD 163296 do not follow the simple power-law dependence expected if these were solely due to free-free radiation. This demonstrates that even at wavelengths as long as 1.3 cm, a significant fraction of the system flux is due to circumstellar dust. The 3.6 and 6 cm fluxes are probably dominated by free-free emission.

The energy distribution of a circumstellar dust disk is governed by its temperature profile, the density distribution and the dust properties (chemical composition and size distribution). Since the circumstellar disks of AB Aur and HD 163296 stars are expected to be passive (Waters & Waelkens 1998) and the properties of the central stars are nearly identical, the temperature profiles in the disks are expected to be similar as well. One possibility to explain the different sub-mm to mm slope for AB Aur and HD 163296 could be a much flatter density distribution for HD 163296. However, with a standard sub-mm dust emissivity ($\beta = 2$) the inferred dust mass for HD 163296 would become implausibly large. A better explanation may be that the dust properties of AB Aur and HD 163296 are different, a fact already concluded independently from the ISO spectra. To be able to radiate efficiently, dust particles must have a size similar to (or larger than) the wavelength, pointing to the existence of a population of mm- to cm-sized cold dust grains in the circumstellar environment of HD 163296, whereas those in AB Aur must be micron-sized. The ISO spectrum of HD 163296 also contains warm (≈ 800 K) dust, suggesting a significant lack of emission from dust of intermediate temperatures.

5. Discussion and conclusions

We have shown that the main difference between the AB Aur and HD 163296 systems is that HD 163296 contains a population of very large (mm to cm-sized), cold, partially crystalline, dust grains, which is absent in AB Aur. AB Aur contains a population of small dust grains (PAHs), which is absent in HD 163296. In view of the fact that the stellar parameters are nearly identical except for stellar rotation, these differences are remarkable. This must mean that either the evolution of the dust composition in protoplanetary disks happens within the error in the age determination of both systems (2^{+2}_{-1} Myr for AB Aur vs. 4^{+4}_{-2} Myr for HD 163296; van den Ancker et al. 1998), or that the evolution of the dust is dominated by external factors.

We have also shown that in AB Aur and HD 163296 iron oxide is a constituent of the circumstellar dust mixture and can also be responsible for the observed excess emission near $3 \mu\text{m}$. Since the near-infrared excess exhibited by our programme stars is by no means unusual for a Herbig Ae/Be star,

this means that the same applies for the entire group of Herbig stars. Therefore the results of models attributing this near infrared excess emission to very hot dust from an actively accreting disk (e.g. Hillenbrand et al. 1992) must be regarded with some caution. The case of HD 163296 demonstrates that infrared broad-band photometry can be completely dominated by emission from solid-state features, which must also be taken into account in any future modelling of the energy distributions of Herbig stars.

The detection of PAHs in AB Aur shows that ground-based surveys (e.g. Brooke et al. 1993) have underestimated the fraction of Herbig stars containing PAHs. The case of HD 163296 shows that the fraction of Herbig stars showing PAH emission will not go up to 100%, so models depending on the presence of very small dust grains to explain the observed near-infrared excess in Herbig Ae/Be stars (Natta et al. 1993; Natta & Krügel 1995) will not be successful in all cases. We believe iron oxide to be a more plausible explanation for this near-infrared excess.

It is difficult to attribute the absence of the $3.29\ \mu\text{m}$ feature in AB Aur to an unusual temperature of the PAHs. Since the 6.2 and $7.7\ \mu\text{m}$ C–C stretches are strong, while the bands due to C–H bonds are weak or absent, a more promising possibility seems a very low hydrogen covering factor of the PAHs in AB Aur or the presence of a population of large (> 100 C atoms) PAHs (Schutte et al. 1993). If the new $15.9\ \mu\text{m}$ UIR band in AB Aur is also caused by PAHs, this suggests that it is also due to a C–C bond.

To gain more insight in the evolution of dust in protoplanetary disks, it is useful to compare the spectra presented here to those of other Herbig Ae stars. Except for the absence of crystalline material, the AB Aur spectrum and energy distribution are nearly identical to those of its older counterpart HD 100546 (Malfait et al. 1998). In the case of AB Aur ($2.5\ M_{\odot}$), any possible crystallization of circumstellar dust must therefore occur at a stellar age older than 2×10^6 years. The differences between HD 100546 and HD 163296 are larger: the crystalline dust in HD 100546 is much more prominent than that in HD 163296 and the population of large cold dust grains seen in HD 163296 is absent in HD 100546.

As these cases of AB Aur, HD 163296 and HD 100546 demonstrate, the age of the central star and the degree of crystallization do not show a one to one correspondence, but the processes of grain growth and crystallization in protoplanetary disks are also not necessarily coupled. Studying a larger sample of Herbig Ae/Be stars might shed more light on what causes this large observed diversity in dust properties in systems which appear very similar in other aspects.

Acknowledgements. This paper is based on observations with ISO, an ESA project with instruments funded by ESA Member States (especially the PI countries: France, Germany, the Netherlands and the United Kingdom) and with the participation of ISAS and NASA and on observations collected at the European Southern Observatory, La Silla, Chile. The authors would like to thank the SWS IDT for their help with the SWS observations and Norman Trams and Michelle Creech-Eakman for their help with the LWS observations. Koen Mal-

fait and Xander Tielens are gratefully acknowledged for reading of the manuscript of this paper prior to publication.

References

- Berrilli, F., Corciulo, G., Ingrassio, G., Lorenzetti, D., Nisini, B., Strafella, F. 1993, *ApJ* 398, 254
- Berrilli, F., Lorenzetti, D., Saraceno, P., Strafella, F. 1987, *MNRAS* 228, 833
- Bertie, J.B. Labbé, H.J., Whalley, B. 1969, *J. Chem. Phys.* 50, 4501
- Bjorkman, K.S. et al. 1995, *BAAS* 27, 1319
- Böhm, T., Catala, C. 1993, *A&AS* 101, 629
- Böhm, T., Catala, C. 1995, *A&A* 301, 155
- Böhm, T., Catala, C., Donati, J.F. et al. 1996, *A&AS* 120, 431
- Bouret, J.C., Catala, C., Simon, T. 1997, *A&A* 328, 606
- Brooke, T.Y., Tokunaga, A.T., Strom, S.E. 1993, *AJ* 106, 656
- Brown, D.A., Pérez, M.R., Yusef-Zadeh, F. 1993, *AJ* 106, 2000
- Catala, C., Simon, T., Praderie, F., Talavera, A., Thé, P.S., Tjin A Djie, H.R.E. 1989, *A&A* 221, 273
- Clegg, P.E., Ade, P.A.R. et al. 1996, *A&A* 315, L38
- Cohen, M. 1980, *MNRAS* 191, 499
- Cohen, M., Schwartz, R.D. 1976, *MNRAS* 174, 137
- de Graauw, Th., Haser, L.N. et al. 1996, *A&A* 315, L49
- Di Francesco, J., Evans, N.J., Harvey, P.M., Mundy, L.G., Butner, H.M. 1998, *ApJ* 509, 324
- Dorschner, J., Begemann, B., Henning, Th., Jäger, C., Mutschke, H. 1995, *A&A* 300, 503
- Grady, C.A., Pérez, M.R., Talavera, A. et al. 1996, *A&AS* 120, 157
- Grady, C.A., Pérez, M.R., Bjorkman, K.S., Massa, D. 1999, *ApJ* 511, 925
- Gray, R.O., Corbally, C.J. 1998, *AJ* 116, 2530
- Güdel, M., Benz, A.O., Catala, C., Praderie, F. 1989, *A&A* 217, L9
- Halbedel, E.M. 1996, *PASP* 108, 833
- Henning, Th., Begemann, B., Mutschke, H., Dorschner, J. 1995, *A&AS* 112, 143
- Henning, Th., Burkert, A., Launhardt, R., Leinert, C., Stecklum, B. 1998, *A&A* 336, 565
- Hillenbrand, L.A., Strom, S.E., Vrba, F.J., Keene, J. 1992, *ApJ* 397, 613
- Jäger, C., Molster, F.J., Dorschner, J., Henning, Th., Mutschke, H., Waters, L.B.F.M. 1998, *A&A* 339, 904
- Kessler, M.F., Steinz, J.A., Anderegg, M.E., Clavel, J., et al. 1996, *A&A* 315, L27
- Malfait, K., Waelkens, C., Waters, L.B.F.M., Vandenbussche, B., Huygen, E., de Graauw, M.S. 1998, *A&A* 332, L25
- Malfait, K., Waelkens, C., Bouwman, J., de Koter, A., Waters, L.B.F.M. 1999, *A&A* 345, 181
- Mannings, V. 1994, *MNRAS* 271, 587
- Mannings, V., Sargent, A.I. 1997, *ApJ* 490, 792
- Marsh, K.A., van Cleve, J.E., Mahoney, M.J., Hayward, T.L., Houck, J.R. 1995, *ApJ* 451, 777
- Merrill, P.W., Burwell, C.G. 1933, *ApJ* 78, 87
- Millan-Gabet, R., Schloerb, F.P., Traub, W.A., Malbet, F., Berger, J.P., Bregman, J.D. 1999, *ApJ* 513, L131
- Natta, A., Krügel, E. 1995, *A&A* 302, 849
- Natta, A., Prusti, T., Krügel, E. 1993, *A&A* 275, 527
- Pogodin, M.A. 1994, *A&A* 282, 141
- Schutte, W.A., Tielens, A.G.G.M., Allamandola, L.J. 1993, *ApJ* 415, 397
- Sitko, M.L. 1981, *ApJ* 247, 1024

- Sitko, M.L., Grady, C., Lynch, D.K., Russell, R.W., Hanner, M.S. 1999, *ApJ* 510, 408
- Skinner, S.L., Brown, A., Stewart, A.T. 1993, *ApJS* 87, 217
- Sorrell, W.H. 1990, *ApJ* 361, 150
- Strom, S.E., Strom, K.E., Yost, J., Carrasco, L., Grasdalen, G. 1972, *ApJ* 173, 353
- Thé, P.S., Felenbok, P., Cuypers, H., Tjin A Djie, H.R.E. 1985, *A&A* 149, 429
- van den Ancker, M.E., Thé, P.S., Tjin A Djie, H.R.E., Catala, C., de Winter, D., Blondel, P.F.C., Waters, L.B.F.M. 1997, *A&A* 324, L33
- van den Ancker, M.E., de Winter, D., Tjin A Djie, H.R.E. 1998, *A&A* 330, 145
- van den Ancker, M.E., Volp, A.W., Pérez, M.R., de Winter, D. 1999, *Inf. Bull. Var. Stars* 4704, 1
- Waters, L.B.F.M., Waelkens, C. 1998, *ARA&A* 36, 233
- Weaver, W.B., Jones, G. 1992, *ApJS* 78, 239
- Wesselius, P.R., van Duinen, R.J., de Jonge, A.R.W., Aalders, J.W.G., Luinge, W., Wildeman, K.J. 1982, *A&AS* 49, 427